

whether all interaction effects are zero or whether all levels of  $A$  have the same effect. A decision on whether to reject the hypothesis is based on examination of the ratio of the goodness-of-fit parameter for the two least-squares estimates; this ratio is tested as the usual variance ratio  $F$ .

The actual calculations were carried out by a general computer program HANOVA, available on request from WCH. A further discussion of the model may be found elsewhere (Hamilton, 1964, for example.)

The experimental contributions of J. L. Bernstein, K. Knox, N. R. Stemple and P. Mackie to various parts of this project are gratefully acknowledged. The work

of some of the participating laboratories was supported by the National Science Foundation (Contract no. GP3864), the United States Atomic Energy Commission and the National Institutes of Health—National Institute of Dental Research (Grant no. DEO1912-04).

#### References

- ABRAHAMS, S. C. (1965). *Acta Cryst.* **18**, 926.  
 HAMILTON, W. C. (1964). *Statistics in Physical Science*. New York: Ronald Press.  
 HAMILTON, W. C., ROLLETT, J. S. & SPARKS, R. A. (1965). *Acta Cryst.* **18**, 129.  
*International Tables for X-Ray Crystallography* (1962). Vol. III, p. 164. Birmingham: Kynoch Press.

*Acta Cryst.* (1967). **22**, 6

## Small-Angle X-ray Scattering by Rods and Sheets: The Interpretation of Line-Collimation Results

BY R. E. BURGE AND J. C. DRAPER

*Department of Physics, University of London, Queen Elizabeth College, Campden Hill Road, London W8, England*

(Received 6 April 1966 and in revised form 21 June 1966)

The conditions are examined under which direct interpretation is possible of small-angle intensity data for isotropic solutions of long rods and thin discs collected with the use of infinite line collimation conditions and on an absolute scale. It is shown by extensive computer calculations, using five different rod models and three different disc models, that in all cases where data obtained under point collimation conditions can be unequivocally interpreted (*i.e.* free of dependence on a theoretical model) in terms of the number of electrons per unit length (area) of rods (discs) and the appropriately defined radius of gyration, the very small-angle infinite line collimation results can be used directly to give the same information.

The effects of the finite length of rods and finite area of discs are considered and the conditions analysed where the measured scattering may be interpreted as if the rods were very long and the discs were of very large area.

### Introduction

Kratky and co-workers and Luzzati and co-workers (for reviews see Kratky, 1963; Luzzati, 1963) have discussed the small-angle X-ray scattering method as applied to macromolecular solutions where the intensity of scattering is assessed on an absolute scale, *i.e.* relative to the energy of the incident beam.

The intensity of X-rays scattered by a dilute, isotropic, macromolecular solution depends on the cross-section of the X-ray beam at the specimen. Cases that have been considered are point collimation and both finite and infinite line collimation (for references see Chu & Creti, 1965). Scattering results are normally obtained with slit collimation and for the purposes of interpretation the results are corrected back to point focus conditions by numerical methods. Luzzati (1958, 1960), however, showed that results obtained with the use of infinite line focus conditions at the specimen

could, for spherical and rod-like particles, be interpreted directly. It was decided in the present work to examine further the direct interpretation of infinite line-focus data from rods and to consider sheets also because of work in progress in this laboratory on bacterial flagella and bacterial cell walls.

Luzzati (1960) interprets the scattering by rods under line collimation conditions by using a rod-model with a given distribution of electron density perpendicular to the rod axis and by evaluating the differences between the predictions of the model and the experimental results. It is not clear in the formulation of the problem as used by Luzzati (1960), first how far the physical parameters deduced for the rods reflect the model used and, second, whether to interpret line-collimation results on the basis of any other rod model makes mandatory their conversion into data appropriate to point collimation conditions. The calculations reported here are addressed to these two problems in

connexion with rods and also to the comparable problems connected with sheets. The discussion of the X-ray scattering by sheets is made in terms of a thin circular disc of large surface area.

The approach we have adopted for rods is to take five models of rigid cylindrical rods which are as different as possible (Table 1) and to determine individually for each condition of collimation how far and under what experimental conditions the intensities of scattering for the five models (calculated with the same values of mass per unit length  $\mu$  and radius of gyration  $R_c$ ) could be interpreted in terms of the known values of  $\mu$  and  $R_c$ . The rod models were chosen partly for their potential value in interpreting results and partly for expediency in calculation (the Maxwellian rod is in the second category). In a similar manner the intensities scattered by discs of three types (Table 2) with the same thickness and mass per unit area are compared for point and infinite-line collimation conditions. It was also found necessary to investigate the effects on the angular dependence of the scattering of finite rod length and finite disc diameter.

It should be noted that the angular range of application of this work is at larger angles than those at which the universal Guinier exponential scattering law – which is expressed in terms of the radius of gyration with respect to the centre of gravity of a particle – is valid. The radii of gyration appropriate to this work are defined in the next section (see also Guinier & Fournet, 1955).

### Theoretical

#### General

Consider a right circular cylinder of radius  $R$  and length  $L$ . Let the orthogonal axes  $r$  and  $z$  be in the directions of  $R$  and  $L$  respectively. If  $L \gg 2R$  this figure behaves as a rigid rod and if  $L \ll 2R$  as a rigid circular disc. Let the particles (rods or discs) in solution be randomly orientated with respect to the incident X-ray beam and the solution be sufficiently dilute for the

particles to scatter independently. Let each particle contain a total of  $m$  electrons. The electron density of the solvent is  $\rho_0$  ( $\text{e} \cdot \text{\AA}^{-3}$ ), the electronic partial specific volume of the solute is  $\psi$  ( $\text{\AA}^3 \cdot \text{e}^{-1}$ ) and the electronic concentration of the solute is  $c_e$  (number of electrons in solute/number of electrons in solution).

Following Luzzati (1960) the ‘reduced’ intensity of scattering  $i_n(s)$  at an angle  $2\theta$  to a *point-like* beam incident on the specimen, expressed as a fraction of the energy of that beam, is given by:

$$i_n(s) = c_e m (1 - \rho_0 \psi)^2 F(s) \quad (1)$$

where  $s = 2 \sin \theta / \lambda$  and each particle has a scattering factor  $F(s)$ .

$F(s)$  in the general case is given by Fournet (1951) as:

$$F(s) = \frac{1}{m^2} \int_0^{\pi/2} \left[ \int_r \int_z \rho(r, z) 2\pi r \cos(hz \cos \theta) \times J_0(hr \sin \theta) dr dz \right]^2 \sin \theta d\theta \quad (2)$$

where  $J_0$  is a Bessel function of zero order,  $h = 2\pi s$ , and the distribution of electron density is given by  $\rho(r, z)$ .

For infinite-line collimation conditions the general expression for the ‘reduced’ intensity of scattering referred to the energy of the main beam is (Guinier & Fournet, 1955; Luzzati, 1960):

$$j_n(s) = c_e m (1 - \rho_0 \psi)^2 \mathcal{F}(s) \quad (3)$$

where

$$\mathcal{F}(s) = 2 \int_0^{\infty} F(s^2 + t^2)^{\frac{1}{2}} dt \quad (4)$$

In equations (1)–(4),  $F(s)$  and  $\mathcal{F}(s)$  stand for general values of the point and line collimation scattering factors; they are defined below for particular cases.

#### Scattering by rigid rods

The parameters describing the five rod models used to evaluate equations (1)–(4) are given in Table 1.  $R_c$  is the radius of gyration of the rod about its long axis.

Table 1. Description of rod models

Type of rod	$q(r, z)$	$R_c^2$	Notation for scattering factor (point focus : line focus)
Plain	constant	$R^2/2$	$F(s); \mathcal{F}(s)$
General plain	$q(r) = A \begin{cases} r=R_1 \\ r=0 \end{cases}$ $= B \begin{cases} r=R \\ r=R_1 \end{cases}$	$\frac{R^2}{2} \left[ \frac{(A-B)q^4 + B}{(A-B)q^2 + B} \right]$  $(q = R_1/R)$	$G(s); \text{—}$
Gaussian*	$q(r) = Ae^{-ar^2}$	$1/a$	$F'(s); \mathcal{F}'(s)$
General Gaussian	$q(r) = Ae^{-ar^2} + Be^{-br^2}$	$\frac{A/a^2 + B/b^2}{A/a + B/b}$	$G'(s); \mathcal{G}'(s)$
Maxwell	$q(r) = Ar^2e^{-ar^2}$	$2/a$	$M(s); \mathcal{M}(s)$

\* This is the density function used implicitly by Luzzati (1960).

(i) *Point collimation*

Equation (2) was evaluated for the five types of rod for rods of any length. Numerical calculations for this general case were made only for plain and Gaussian rods but all the rod-types were considered in the special cases  $L \rightarrow \infty$ . The expressions used for calculation are:

$$F(s) = \int_0^{\pi/2} \frac{\sin^2(\pi L s \cos \theta)}{(\pi L s \cos \theta)^2} \cdot \frac{4J_1^2(2\pi R s \sin \theta)}{(2\pi R s \sin \theta)^2} \times \sin \theta d\theta, \quad (5)$$

where  $J_1$  is a first order Bessel function.

$$F(s)_{L \rightarrow \infty} = \frac{1}{2Ls} \cdot \frac{4J_1^2(2\pi R s)}{(2\pi R s)^2}. \quad (6)$$

$$G(s)_{L \rightarrow \infty} = \frac{1}{2Ls} \cdot \frac{4}{[(A-B)q^2 + B]^2} \times \left\{ \frac{BJ_1(2\pi R s)}{2\pi R s} + \frac{(A-B)q^2 J_1(2\pi q R s)}{2\pi q R s} \right\}^2. \quad (7)$$

$$F'(s) = \int_0^{\pi/2} \frac{\sin^2(\pi L s \cos \theta)}{(\pi L s \cos \theta)^2} \cdot \exp(-2\pi^2 s^2 R_c^2 \sin^2 \theta) \times \sin \theta d\theta. \quad (8)$$

$$F'(s)_{L \rightarrow \infty} = \frac{1}{2Ls} \cdot \exp(-2\pi^2 s^2 R_c^2). \quad (9)$$

$$G'(s)_{L \rightarrow \infty} = \frac{1}{2Ls} \cdot \frac{1}{(A/a + B/b)^2} \times \left[ \frac{A}{a} \exp\left(-\frac{\pi^2 s^2}{a}\right) + \frac{B}{b} \exp\left(-\frac{\pi^2 s^2}{b}\right) \right]^2. \quad (10)$$

$$M(s)_{L \rightarrow \infty} = \frac{1}{2Ls} \cdot \exp(-\pi^2 s^2 R_c^2) \left[ 1 - \frac{\pi^2 s^2 R_c^2}{2} \right]^2. \quad (11)$$

Equations (5) and (6) are given respectively by Fournet (1951) and Guinier & Fournet (1955).

In terms of  $i_n(s)$  from equation (1), writing  $\mu = m/L$  the electronic 'mass' per unit length, equations (6), (7), (9), (10) and (11) give the relationship:

$$[\mu]_{L \rightarrow \infty} = \frac{2[s i_n(s)]_{s \rightarrow 0}}{c_e(1 - \rho_0 \psi)^2}. \quad (12)$$

Equation (12) is based on equations which are valid for  $s \gg 1/L$  and some care is necessary in the extrapolation to zero scattering angle; this point is dealt with by Luzzati (1960). Equations (6), (9), and (11) provide a simple method of determining  $R_c$  since in the three cases

$$[s i_n(s)]_{\text{small } s} \rightarrow \frac{1}{2} c_e \mu (1 - \rho_0 \psi)^2 (1 - 2\pi^2 R_c^2 s^2). \quad (13)$$

For the long general plain and long general Gaussian rods the slope of a graph of  $s i_n(s)$  versus  $s^2$  is not simply related to  $R_c$  (see values in Table 1).

(ii) *Infinite line collimation*

For the cases relevant to equations (5), (6), (7), (8) values of the scattering factors for line collimation

conditions can only be produced by numerical integration following the substitution of the point collimation parameters into equation (4). For the long Gaussian, long general Gaussian and long Maxwellian rods, however, values of the line-collimation scattering factors can be put into closed form:

$$\mathcal{F}'(s)_{L \rightarrow \infty} = \frac{1}{2L} \exp(-\pi^2 R_c^2 s^2) K_0(\pi^2 R_c^2 s^2) \quad (14)$$

where  $K_0$  is a Bessel function of imaginary argument (Watson, 1952). Equation (14) was first given by Luzzati (1960).

$$\mathcal{G}'(s)_{L \rightarrow \infty} = \frac{1}{2L} \cdot \frac{1}{(A/a + B/b)^2} \left\{ \frac{A^2}{a^2} \exp\left(-\frac{\pi^2 s^2}{a}\right) \times K_0\left(\frac{\pi^2 s^2}{a}\right) + \frac{B^2}{b^2} \exp\left(-\frac{\pi^2 s^2}{b}\right) K_0\left(\frac{\pi^2 s^2}{b}\right) + \frac{2AB}{ab} \exp\left[\frac{-\pi^2}{2} \left(\frac{1}{a} + \frac{1}{b}\right) s^2\right] \times K_0\left[\frac{\pi^2}{2} \left(\frac{1}{a} + \frac{1}{b}\right) s^2\right] \right\} \quad (15)$$

$$\mathcal{M}(s)_{L \rightarrow \infty} = \frac{1}{2L} \exp\left(-\frac{\pi^2 R_c^2 s^2}{2}\right) \left\{ K_0\left(\frac{\pi^2 R_c^2 s^2}{2}\right) + \frac{\pi^{3/2}}{4} R_c s W_{1,1}(\pi^2 R_c^2 s^2) - \pi^{3/2} W_{3/2,3/2}(\pi^2 R_c^2 s^2) \right\} \quad (16)$$

where  $W_{k,m}(x)$  is a Whittaker confluent hypergeometric function (Whittaker & Watson, 1962, p. 340).

(iii) *Effect of finite rod length on scattering factors*

The scattering factors for point collimation conditions are derived for  $L \rightarrow \infty$  from equations (5) and (8) by noting that  $\sin^2(\pi L s \cos \theta)/(\pi L s \cos \theta)^2$  behaves as a peak function and is negligibly small except when  $\cos \theta \rightarrow 0$ . For shorter rods a second approximation to, for example, equation (8) may be taken (see also Stokes, 1957) as follows:

$$F'(s)_{L/R_c \gg 1} = \exp(-2\pi^2 R_c^2 s^2) \left[ \frac{1}{2Ls} - \frac{1}{2(\pi L s)^2} - \frac{1}{4} \times \frac{\sin(2\pi L s)}{(\pi L s)^3} + \frac{1}{4} \cdot \frac{\cos(2\pi L s)}{(\pi L s)^4} + \dots \right]. \quad (9a)$$

Taking the first two terms of the expansion, we have from equation (4):

$$\mathcal{F}'(s)_{L/R_c \gg 1} = \frac{1}{2L} \left\{ \exp(-\pi^2 R_c^2 s^2) K_0(\pi^2 R_c^2 s^2) - \frac{R_c/L}{\pi R_c s} \operatorname{Erfc}(\sqrt{2\pi R_c s}) \right\}, \quad (14a)$$

where

$$\operatorname{Erfc}(x) = 1 - \frac{2}{\pi^{1/2}} \int_0^x e^{-t^2} dt.$$

An equation similar to (14a) but for flexible rods was given by Witz, Hirth & Luzzati (1965) and some calcu-

lations based on equation (14a) but without its derivation are given by Luzzati, Witz & Timasheff (LWT, 1961).

In a similar manner equations for the scattering factors for plain and Maxwellian rods for  $L/R_c \gg 1$  can readily be formulated.

*Scattering by rigid discs*

The parameters describing the three disc models are given in Table 2. The values of  $R_c$  are referred to the plane passing through the centre of the disc and parallel to its surface.

(i) *Point collimation*

Equation (5) is applicable to the determination of  $F(s)$  for a plain disc of any radius. For a plain disc of large radius we have for  $s \gg 1/R$ .

$$F(s) = \frac{1}{\pi R^2} \cdot \frac{1}{2\pi s^2} \cdot \frac{\sin^2(\pi Ls)}{(\pi Ls)^2}; \quad (17)$$

also

$$G(s) = \frac{1}{\pi R^2} \cdot \frac{1}{2\pi s^2} \cdot \frac{1}{[HB + H_1(A - B)]^2} \times \left[ \frac{HB \sin(2\pi Hs)}{2\pi Hs} + H_1(A - B) \frac{\sin(2\pi H_1s)}{2\pi H_1s} \right]^2 \quad (18)$$

$$F'(s) = \int_0^{\pi/2} \frac{4J_1^2(2\pi Rs \sin \theta)}{(2\pi Rs \sin \theta)^2} \times \exp(-4\pi^2 R_c^2 s^2 \cos^2 \theta) \sin \theta d\theta. \quad (19)$$

$$F'_{R \rightarrow \infty}(s) = \frac{1}{\pi R^2} \cdot \frac{1}{2\pi s^2} \exp(-4\pi^2 R_c^2 s^2). \quad (20)$$

From equations (17), (18), and (20) and equation (1), the electronic 'mass' per unit area  $M = m/\pi R^2$  is given by:

$$M = \frac{2\pi [s^2 i_n(s)]_{s \rightarrow 0}}{c_e(1 - \rho_0 \psi)^2} \quad (21)$$

subject to certain conditions relating to the extrapolation (Luzzati, 1960). For small angles of scattering  $R_c$  can be determined from equations (17) and (20) since

$$2\pi [s^2 i_n(s)]_{\text{small } s} \rightarrow c_e M (1 - \rho_0 \psi)^2 [1 - 4\pi^2 R_c^2 s^2], \quad (22)$$

but no such simple relationship for  $R_c$  follows from the small-angle behaviour of equation (18).

(ii) *Infinite line collimation*

The line collimation scattering factors for plain discs of finite area, for infinite plain and layered discs, and finite Gaussian discs are given by substituting equations (5), (17), (18) and (19) into equation (4) and are not readily expressed in closed form. For the Gaussian disc of large radius we have

$$\mathcal{F}'(s) = \frac{1}{\pi R^2} \cdot \frac{[1 - \text{Erf}(2\pi R_c s)]}{2s} \quad (23)$$

where

$$\text{Erf}(\pi) = 2/\pi^{\frac{1}{2}} \int_0^{\pi} e^{-t^2} dt.$$

It follows from equations (3) and (23) that in this case

$$M = \frac{2 [s j_n(s)]_{s \rightarrow 0}}{c_e(1 - \rho_0 \psi)^2} \quad (24)$$

and  $R_c$  is given by

$$[s j_n(s)]_{\text{small } s} \rightarrow \frac{c_e M (1 - \rho_0 \psi)^2}{2} \left( 1 - \frac{4\pi R_c s}{\sqrt{\pi}} \right). \quad (25)$$

**Calculations\***

*Rigid rods*

$F(s)$  for plain rods was evaluated from equation (5) by Gaussian quadrature (see also Malmon, 1957) for ranges of  $2sR$  between zero and about 3.5 for  $L/2R = 10, 20, 100$ . For the subsequent calculations of  $\mathcal{F}(s)$  from the infinite integral in equation (4), values of  $F(s)$  over a wide angular range were required. In the range of  $s$  chosen the numerical value of  $F(s)$  fell by a factor of  $10^6$ .

Calculations of  $F'(s)$  for Gaussian rods for comparison with  $F(s)$  for plain rods were made on the assumption that the two types of rod had the same value of  $R_c$ . Thus equation (8) was evaluated for  $L/2\sqrt{2}R_c = 20, 100$ .

The line-collimation function  $\mathcal{F}(s)$  was calculated for plain rods, using equation (4) for the angular

\* Numerical values are available on application to the authors.

Table 2. *Description of disc models*

Type of disc	$\rho(r, z)$	$R_c^2$	Notation for scattering factor (point focus : line focus)
Plain	Constant	$L^2/12$	$F(s); \mathcal{F}(s)$
Layered	$\rho(z) = A \begin{cases} z = +H_1 \\ \\ z = -H_1 \end{cases}$ $= B \begin{cases} z = \pm H \\ \\ z = \pm H_1 \end{cases}$	$\frac{AH_1^3 + B(H^3 - H_1^3)}{3[AH_1 + B(H - H_1)]}$  ( $L = 2H$ )	$G(s); -$
Gaussian	$\rho(z) = Ae^{-az^2}$	$1/2a$	$F'(s); \mathcal{F}'(s)$

range  $0 \leq 2Rs \leq 1.9$  and for  $L/2R=20, 100$ . This was accomplished by a standard numerical procedure. Errors of integration were reduced to less than 1% for all values of  $2Rs$  considered (for small  $s$  values to less than 0.1%). The function  $\mathcal{F}(s) \cdot L$  for plain rods of finite length is plotted in Fig.1 for  $L/2R=20, 100$ . In addition, for comparison, in Fig.1 are plotted (i)  $\mathcal{F}(s) \cdot L$  for long plain rods produced by numerical

integration of equation (4), after substitution from equation (6), (ii)  $\mathcal{F}'(s) \cdot L$  for long Gaussian rods

evaluated from equation (14), (iii)  $\mathcal{M}(s) \cdot L$  for long

Maxwellian rods evaluated from equation (16).

$\mathcal{F}'(s)$  for finite Gaussian rods was evaluated from equations (4) and (8) and the effects of finite rod length for plain and Gaussian rods are brought out in Fig.2 where the parameter

$$d(s) = \frac{j_n(s)_{L \rightarrow \infty} - j_n(s)_{L/2R}}{j_n(s)_{L/2R}}$$

for a plain rod and the equivalent parameter  $d'(s)$  for a Gaussian rod are plotted against  $2Rs$ . For Gaussian rods with  $L/R_c=40\sqrt{2}$  and  $200\sqrt{2}$ ,  $d'(s)$  was evaluated from equations (14) and (14a) for comparison with the exact computer results; these values are also shown in Fig.2.

#### Rigid discs

The shapes chosen for the calculation of  $F(s)$  were specified by  $L/2R=10^{-1}$  and  $3 \times 10^{-1}$ . The line-collima-

tion function  $\mathcal{F}(s)$  was derived from  $F(s)$  in the same way as for rods for plain discs of both shapes with a maximum error of less than 1% for  $Ls < 2$ . Values of  $\mathcal{F}(s) \cdot \pi R^2$  from equations (4) and (5) are shown in Fig.3 for  $L/2R=10^{-1}, 3 \times 10^{-1}$ . In Fig.3 values are also shown of  $\mathcal{F}(s) \cdot \pi R^2$  for a plain disc of large radius

evaluated by the numerical integration of equation (4) after substitution from equation (17).

Calculations for Gaussian discs were restricted to discs of large area and for comparison with the results for large plain discs the radii of gyration of the two shapes were made equal, *i.e.*  $R_c$  for the Gaussian disc was equated to  $L/2\sqrt{3}$ . The function  $\mathcal{F}'(s) \cdot \pi R^2$  [see equation (23)] is shown in Fig.3.

## INTERPRETATION OF EXPERIMENTAL RESULTS: INFINITE LINE COLLIMATION CONDITIONS

### Scattering by rigid rods

#### (a) Effects of finite rod length

LWT (1961) discuss the scattering by short Gaussian rods and show curves effectively of  $\mathcal{F}'(s) \cdot L$  derived from equation 14(a) for  $L/R_c=5, 10$  and claim that at sufficiently large scattering angles the differences between the  $\mathcal{F}'(s) \cdot L$  values for infinitely long and short rods are negligible. That this is not so can be seen from the differences between the two-term approximation to  $\mathcal{F}'(s)$  and the exact computer data shown in Fig.2. Although the minimum  $L/R_c$  value used for calculation

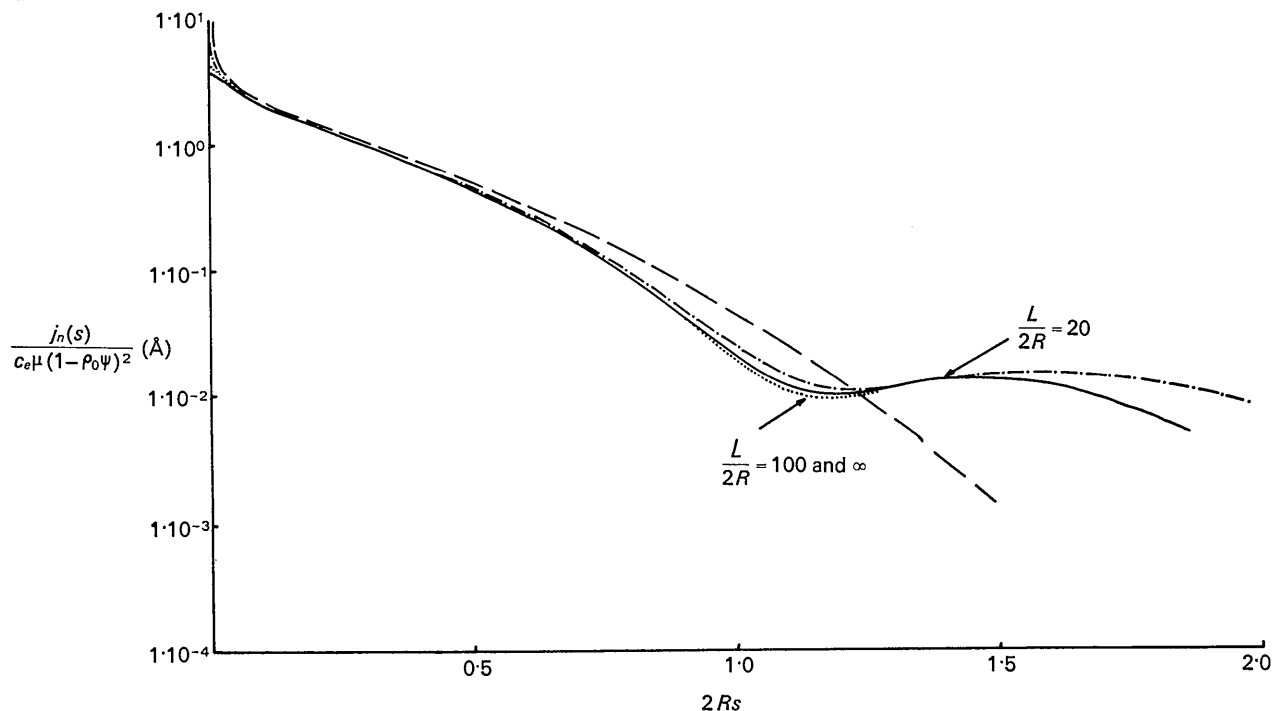


Fig.1. Scattering factors for rods (infinite line collimation). Full and dotted line:  $\mathcal{F}(s) \cdot L$  for plain rods with given value of  $L/2R$ . Dashed line:  $\mathcal{F}'(s) \cdot L$  for infinite Gaussian rod. Chain-dotted line:  $\mathcal{M}(s) \cdot L$  for infinite Maxwellian rod.

was  $40\sqrt{2}$  the dependence of the curves on this ratio indicates that the two-term approximation will be in considerable error for  $L/R_c$  less than about 20. There seems no escape from detailed calculations of the line-focus function  $\mathcal{F}'(s)$  for short rods to carry to completion an interpretation of experimental results on the basis of a Gaussian rod.

Fig. 2 shows that for Gaussian or plain rods, within an accuracy equivalent to that of the measurement of the scattered intensity (perhaps 3–5%), for rods with

$L/2R > 20$  and  $2Rs < \sim 1$  the scattering curves may be interpreted as if the scatterers were infinitely long; only these cases will be considered further.

(b) *Effects of rod model on measured parameters*

(i) *Very small angles*

It follows from equation (4) that in general the  $\mathcal{F}(s)$  values for different rod models will be different. However it is necessary to consider the magnitudes of the

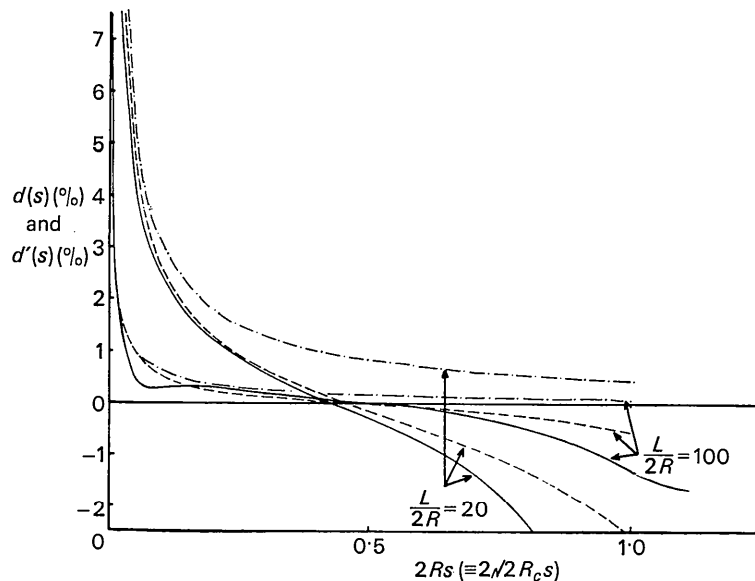


Fig. 2. Effects on scattering factors of finite length of plain and Gaussian rods (see text). Full lines:  $d(s)$  for plain rods from computer data. Dashed lines:  $d'(s)$  for Gaussian rods from computer data. Chain-dotted lines:  $d'(s)$  for Gaussian rods from two-term approximation.

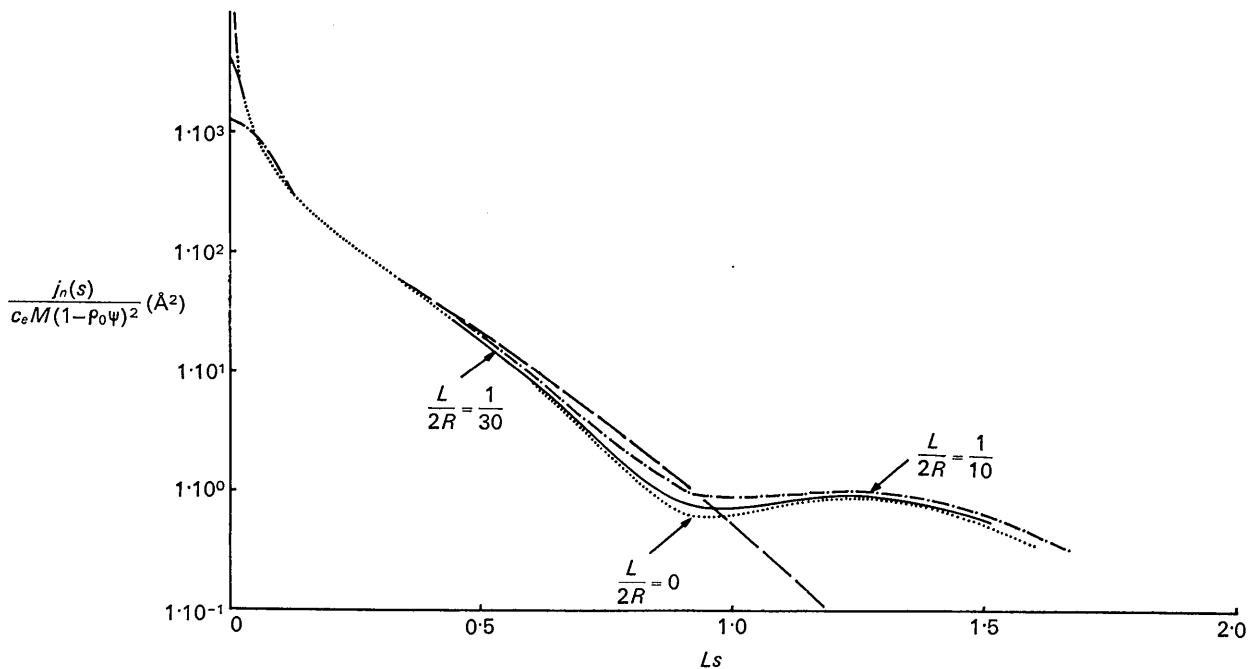


Fig. 3. Scattering factors for discs (infinite line collimation). Full, chain-dotted, and dotted lines:  $\mathcal{F}(s) \cdot \pi R^2$  for plain discs with  $L/2R = 1/30, 1/10, 0$  respectively. Dashed line:  $\mathcal{F}'(s) \cdot \pi R^2$  for Gaussian disc of infinite area.

differences and the angular ranges where the differences occur. Fig. 1 shows that at small values of  $s$  the reduced scattering functions are very similar for long rods with the same length, mass per unit length and radius of gyration. In fact the differences between the numerical values of  $\mathcal{F}(s) \cdot L$  and  $\mathcal{F}'(s) \cdot L$  for  $2Rs < 0.1$  are less than 3% and the values of  $\mathcal{F}(s) \cdot L$  and  $\mathcal{M}(s) \cdot L$  differ

by much less than this in the same angular range. Thus the results for long plain, Gaussian or Maxwellian rods can equally well be interpreted at small  $s$  values by equation (14); for small  $s$  this equation as substituted in equation (3) may be written:

$$j_n(s)_{\text{small } s} \rightarrow -c_e \mu (1 - \rho_0 \psi)^2 [\ln s + \ln R_c + 1.09]. \quad (26)$$

For a general Gaussian rod [equation (15)], the slope at small scattering angles of a line of  $j_n(s)$  plotted against  $-\ln s$  is the same as that given by equation (26) and allows the determination of  $\mu$ . However, the intercept on the  $-\ln s$  axis is not simply related to the radius of gyration. The infinite line collimation equation for a general plain rod was not evaluated but it is expected that its mass per unit length would be given in the same way as for the general Gaussian rod but its  $R_c$  value would not be readily determined.

### (ii) Intermediate angles of scattering

The method given above of interpreting line-focus data concentrates attention on the scattering at  $s < 1/20R \text{ \AA}^{-1}$  and it is of interest to examine the method of interpretation suggested by Luzzati (1960). A number of applications of the Luzzati method have been made, e.g. by Luzzati, Nicolaieff & Masson (1961) (LNM) to the sodium salt of deoxyribonucleic acid and by Luzzati, Cesari, Spach, Masson & Vincent (1961) (LCSMV) to the isotropic phase of poly- $\gamma$ -benzyl-L-glutamate (PLBG).

The Luzzati procedure consists in fitting to the experimental reduced intensity values,  $[j_n(s)]_{\text{expt}}$ , the following function which is derived from the case of an infinite Gaussian rod [see equation (14)].

$$[j_n(s)]_{\text{expt}} = c_e \mu (1 - \rho_0 \psi)^2 \cdot \frac{1}{2} \exp(-\pi^2 \alpha^2 s^2) \times K_0(\pi^2 \alpha^2 s^2) + g(s) \quad (27)$$

The values of  $[j_n(s)]_{\text{expt}}$  are plotted against  $\log s$  on the same graph as a curve of  $\log \left[ \frac{1}{2} \exp(-\pi^2 s^2) K_0(\pi^2 s^2) \right]$  against  $\log s$ . The agreement between the curves is tested by orthogonal translations of the experimental curve to coincide with the known function. To reduce the effects of inter-rod interference on the interpretation more account is taken of the agreement between the curves for solutions of low concentration and for large (in terms of small angle scattering) scattering angles (see LNM, 1961). In all cases studied by the Luzzati group  $g(s)$  has been found to be negligibly small and  $\alpha$  has been taken to be equal to  $R_c$ ; this has given rise to the assumption that the determined values

of  $\mu$  and  $R_c$  based on a Gaussian rod and without extrapolations to very small scattering angles are unique.

To show that the Gaussian rod solution is not unique as determined from the scattering at intermediate  $s$  values and in the presence of experimental errors, curves of  $\log [j_n(s)/c_e \mu (1 - \rho_0 \psi)^2]$  were plotted against  $\log s$  for infinite plain, Gaussian and Maxwellian rods with the same value for  $\mu$  and for  $R_c = 4.7 \text{ \AA}$  as for PLBG.

At angles less than  $s \sim 10^{-2} \text{ \AA}^{-1}$  the curves converged as expected. At higher angles to superimpose the curve for the plain rod on that for the Gaussian rod required changes in both  $\mu$  and  $R_c$ . If the fit is made at  $s = 5 \times 10^{-2} \text{ \AA}^{-1}$  then the ratios arise  $\mu(\text{Gaussian})/\mu(\text{plain}) = 1/0.79$  and  $R_c(g)/R_c(p) = 1/1.08$ . For  $s = 4 \times 10^{-2} \text{ \AA}^{-1}$  the ratios were  $\mu(g)/\mu(p) = 1/0.87$  and  $R_c(g)/R_c(p) = 1/1.06$ . Intermediate values of the ratios were found when the results for the Gaussian and Maxwellian rods are compared.

It seems to us that to interpret the scattering results from rigid rods a combination is required of an extrapolation to small scattering angles to determine  $\mu$  and  $R_c$  free of the precise nature of the rod model followed by an assessment of the degree of fit, over the angular range of the experiments, of the intensity calculated for various rod models.

### Scattering by rigid discs

#### (a) Effects of finite disc area

It is clear from Fig. 3 that for  $L/2R < \frac{1}{30}$  the difference in the intensity scattered per unit area by discs of finite and infinite radius is negligible for  $Ls < \sim 0.7$ . In most practical cases the ratio  $L/2R$  is expected to be much less than  $\frac{1}{30}$  and only the case of a disc of large area will be considered further.

#### (b) Effects of disc model on measured parameters

It has been shown [equations (24) and (25)] that under line-collimation conditions both  $M$  and  $R_c$  for a Gaussian disc may be determined directly. To assess the different conclusions that might be drawn from using the plain and Gaussian disc models a comparison was made between the numerical values of  $\mathcal{F}(s) \cdot \pi R^2$  and  $\mathcal{F}'(s) \cdot \pi R^2$ . The values were found to differ by

less than 2% within the angular range  $Ls < 0.15$ . In this angular range we have for both models

$$[sj_n(s)]_{\text{small } s} \rightarrow \frac{1}{2} c_e M (1 - \rho_0 \psi)^2 (1 - \sqrt{4\pi/3} Ls). \quad (28)$$

By using this equation,  $M$  and  $R_c$  may therefore be determined free, at least, from the characteristics of the plain or Gaussian disc models. However, just as for general plain and Gaussian rods, analysis shows that for layered discs only  $M$  may be determined free of model dependence; for general values of  $A$  and  $B$  the slope of a graph of  $sj_n(s)$  versus  $Ls$  is not simply related to  $R_c$ .

### Conclusion

It has been shown that the results of two hypothetical scattering experiments on an ideal solution of isotropic long rods with respectively point and infinite-line collimation conditions may be unequivocally interpreted in terms of the same value of mass per unit length regardless of the details of the rod-model used in the interpretation. To overcome the effect of the choice of model when critical experiments such as those to distinguish between the  $\alpha$  and  $3_{10}$  helices are contemplated (LCSMV, 1961) the results show that it is essential to determine  $\mu$  from the very small angle scattering behaviour in the infinite line focus case in contrast to the method described by LNM (1961). For infinite-line collimation the radial density distribution appropriate to the real rod may be deduced, as for point collimation, from the behaviour of the model scattering function and the experimental intensity results at intermediate and large scattering angles. In every case considered where  $R_c$  may be readily determined from point focus results (where the radial density function contains only a single term)  $R_c$  may also be readily determined directly from the infinite line focus data. Similar remarks are valid for the relationships between the point and line focus results for discs.

It seems, therefore, that when there is good reason to suppose from other evidence, e.g. electron microscopy or X-ray diffraction of material in the solid state, that the rods or discs can be adequately described by a simple density function, there is no point in 'correcting' the line focus to point focus data. However, if the density function contains terms in  $A$  and  $B$  (Tables 1 and 2) and a Fourier inversion or a trial and error method to determine their values must be used, it is far simpler to apply these methods to the point focus data and a clear case exists for the 'correction' of the line-focus results.

The similarity between the  $\mathcal{F}(s)$  curves for the different simple rods and different simple discs is due to the form of the  $F(s)$  curves. The point focus functions decrease rapidly with increasing  $s$  and for rods or discs with the same  $R_c$  values are very similar at small scattering angles where the scattered intensity is high. The small-angle values of  $\mathcal{F}(s)$  are therefore relatively insensitive to the fluctuations in  $F(s)$  that occur at intermediate and large angles.

When short rods ( $L/R_c < \sim 20$ ) or discs of small radius, ( $L/2R > \sim \frac{1}{30}$ ) are considered, care must be taken in accounting for the effects on the scattering of

the finite particle size. For the  $L/R_c$  range of rigid rods considered by LWT (1961) the method they advocate for correcting for finite rod length is questionable.

Although the calculations described are for rigid rods and rigid discs, the short X-ray wavelength in relation to the dimensions of particles suitable for examination by the method ensures that the results will be virtually unaffected by the flexibility (not for rods to be confused with a Gaussian chain) of real rods and real sheets.

The angular regions of the line collimation scattering patterns where the nature of the rod or disc model is unimportant are at small scattering angles, e.g. for a rod 10 Å in diameter the region is  $s < 10^{-2}$  Å<sup>-1</sup> and for a disc 100 Å in thickness  $s < 1.5 \times 10^{-3}$  Å<sup>-1</sup>. These angles are well within the angular range open to experiment using cameras that are available commercially.

One of us (JCD) wishes to acknowledge an M.R.C. studentship which was held while part of this work was done. The computations were made on the University of London Atlas computer.

### References

- CHU, B. & CRET, D. M. T. (1965). *Acta Cryst.* **18**, 1083.  
 FOURNET, G. (1951). *Bull. Soc. franç. Minér. Crist.* **74**, 39.  
 GUINIER, A. & FOURNET, G. (1955). *Small-angle Scattering of X-rays*. New York: John Wiley.  
 KRATKY, O. (1963). *Progr. Biophys.* **13**, 105.  
 LUZZATI, V., CESARI, M., SPACH, G., MASSON, F. & VINCENT, J. M. (1961). *J. Mol. Biol.* **3**, 566.  
 LUZZATI, V. (1958). *Acta Cryst.* **11**, 843.  
 LUZZATI, V. (1960). *Acta Cryst.* **13**, 939.  
 LUZZATI, V. (1963). In *X-ray Optics & X-ray Microanalysis*, p. 133. Ed. H. H. Pattee, V. E. Cosslett & A. Engstrom. New York: Academic Press.  
 LUZZATI, V., NICOLAIEFF, A. & MASSON, F. (1961). *J. Mol. Biol.* **3**, 185.  
 LUZZATI, V., WITZ, J. & TIMASHEFF, S. N. (1961). *Colloques Internationaux du Centre National de la Recherche Scientifique*, Editions du Centre, 1962, p. 123.  
 MALMON, A. G. (1957). *Acta Cryst.* **10**, 639.  
 SALUDJIAN, P., & LUZZATI, V. (1966). *J. Mol. Biol.* **15**, 681.  
 STOKES, A. R. (1957). *Proc. Phys. Soc. B*, **70**, 379.  
 WATSON, G. N. (1952). *A Treatise on the Theory of Bessel Functions*. Cambridge University Press.  
 WHITTAKER, E. T. & WATSON, G. N. (1962). *A Course in Modern Analysis*. 4th ed. Cambridge Univ. Press.  
 WITZ, J., HIRTH, L. & LUZZATI, V. (1965). *J. Mol. Biol.* **11**, 613.